Available online at www.sciencedirect.com
ScienceDirect
Journal of Photochemistry and Photobiology A: Chemistry 183 (2006) 15–21
Journal of Photochemistry and Photobiology A:Chemistry
www.elsevier.com/locate/jphotochem

Dye-sensitized solar cells based on crosslinked poly(ethylene glycol) electrolytes

Moon-Sung Kang [a], Jong Hak Kim [b], Jongok Won [c], Yong Soo Kang [d,*]

[a] *Energy Lab, Samsung SDI Corporate R&D Center, 428-5 Gongse-dong, Giheung-gu, Yongin-si, Gyeonggi-do 449-577, Republic of Korea*
[b] *Department of Chemical Engineering, Yonsei University, Seoul 120-749, Republic of Korea*
[c] *Department of Applied Chemistry, Sejong University, Seoul 143-747, Republic of Korea*
[d] *Department of Chemical Engineering, Hanyang University, 17 Haengdang-dong, Seongdong-gu, Seoul 133-791, Republic of Korea*

Received 15 December 2005; accepted 9 February 2006
Available online 6 March 2006

Abstract

The high-energy conversion efficiency in solid-state dye-sensitized solar cells (SDSCs) has been achieved by both the better interfacial contact between solid polymer medium and dye molecules and the higher ionic conductivity of polymer electrolyte. Low molecular weight poly(ethylene glycol) (oligo-PEG, $M_w = 1000$) has been used for the deeper penetration of electrolyte into nanoporous TiO_2 layer and consequently the better interfacial contact, followed by crosslinking terminal –OH groups of oligo-PEG with bifunctional glutaraldehyde. The ionic conductivity for the crosslinked oligo-PEG electrolytes is in the range of 10^{-5} to 10^{-3} S cm^{-1} at room temperature, which is high enough for solar cell applications and is presumably due to the increased intersegmental distance with an addition of the crosslinker as confirmed by WAXS analysis. The best result of the SDSCs is the short circuit current (J_{sc}) of 9.48 mA cm^{-2}, the open circuit voltage (V_{oc}) of 0.64 V, the fill factor (ff) of 0.60 and the overall energy conversion efficiency (η) of 3.64% at 100 mW cm^{-2} (AM 1.5).

Keywords: Dye-sensitized solar cells; Interfacial contact; Polymer electrolyte; Crosslinking

1. Introduction

Dye-sensitized solar cells (DSCs) have attractive features such as high-energy conversion efficiency (i.e. ~11% at 1 sun, AM1.5) and low production cost (of 1/5 compared to those of silicon solar cells) [1–7]. DSCs are composed of a photoelectrode with a thin nanoporous film of TiO_2 particles adsorbed by ruthenium metal–organic dyes, an electrolyte dissolving redox couples (I^-/I_3^-), and a platinum (Pt)-layered counter electrode. The function of such device is based on the injection of electrons from a photo-excited state of dye molecules into the conduction band of TiO_2 nanoparticles [1–11]. A redox couple dissolved in a medium reduces the oxidized dye and functions as the electron carrier between photoelectrode and counter electrode in DSCs. Therefore, an electrolyte containing a suitable redox couple plays a very important part in determining the photovoltaic characteristics and the durability of DSCs. The redox couple has been usually dissolved in a liquid-state organic solvent such as acetonitrile, yielding some problems such as leakage or evaporation of the solvent, and flammability. In this regard, several attempts have been made to substitute liquid electrolytes in DSCs with solid or quasi-solid-state electrolytes [8–10,12–19].

Solid polymer electrolytes (SPEs) have received considerable attention over the last decades because of their potential applications in separation membranes [20–23], solid-state batteries [24,25] and DSCs [8–10]. For a successful application of SPEs in DSCs, high ionic conductivity of SPEs is essential. Poly(ethylene oxide) (PEO) has attracted much scientific attention due to its high polarity to dissolve redox couples and excellent chemical stability. However, the ionic conductivity is rather poor primarily due to its high crystallinity. Therefore, there have been many attempts to modify PEO to increase the ionic conductivity [8–10]. Typical example is to incorporate comonomers or nanoparticle fillers. For example, it has been reported that the ionic conductivity of a polymer electrolyte comprising poly(epichlorohydrin-co-ethylene oxide) (referred to as Epichlomer) with 9 and 0.9% (w/w) of NaI and I_2, respectively, is 1.5×10^{-5} S cm^{-1}, resulting in a high overall energy conversion

* Corresponding author. Tel.: +82 2 2220 2336; fax: +82 2 2296 2969.
E-mail address: kangys@hanyang.ac.kr (Y.S. Kang).

1010-6030/$ – see front matter © 2006 Elsevier B.V. All rights reserved.
doi:10.1016/j.jphotochem.2006.02.013

efficiency of 2.6% at 10 mW cm^{-2}, whereas the corresponding value for neat PEO (M_w = 1,000,000) is 1.65×10^{-6} S cm^{-1} [8]. Another approach for enhancing the conductivity of SPEs is the introduction of inorganic nano-fillers to prevent crystal formation and consequently to enhance the mobility of redox couples [9,10]. For instance, nanocrystalline TiO_2 particles were introduced to PEO/LiI/I_2 electrolyte to prevent crystal formation of PEO, resulting in a high overall energy conversion of 4.2% at 65.6 mW cm^{-2} [9]. These results suggest that the ionic conductivity is an important factor in determining the overall energy conversion efficiency of solid-state DSCs (SDSCs). Recently, moreover, the importance of the interfacial contact between polymer electrolyte and dye-adsorbed semiconductor has been demonstrated [26–28]. Namely, the penetration of electrolytes through the nanopores of photoelectrode is very essential to obtain good photovoltaic performance of DSCs employing polymer electrolytes. Therefore, it was suggested that the radius of gyration (R_g) of polymer chains and the pore diameter should be adequately balanced for deeper penetration of polymer electrolytes into TiO_2 nanopores. The coil size of polymer chains is commonly represented by the radius of gyration, R_g, expressed approximately by $R_g = C(M_w)^{1/2}$, where M_w is the molecular weight in g/mol and $C = 0.063$ nm/(g/mol)$^{1/2}$ for PEO in a good solvent [29]. In the case of PEO or its derivatives, therefore, its molecular weight of several thousands is recommended to prepare highly efficient SDSCs. Since low molecular poly(ether)s such as poly(ethylene glycol) (PEG) and poly(propylene glycol) (PPG) are usually in a liquid-state, their solidification should be followed for preparing SDSCs [26–28]. The use of oligomers to prepare SDSCs is referred to as "Oligomer approach".

In this regard, we have constructed highly efficient SDSCs employing low molecular weight PEG (oligo-PEG, M_w = 1000 g/mol; R_g = 2 nm), followed by crosslinking of terminal –OH groups with glutaraldehyde (GA). Oligo-PEG can be easily penetrated into the dye-adsorbed nanoporous TiO_2 layer due to its small coil size compared to the average pore diameter of nanopores in the layer, and the mechanical stability can also be maintained by crosslinking. Thus, the crosslinked polymer electrolytes can provide excellent interfacial contact between electrolyte and dye molecules.

2. Experimental

2.1. DSC preparation

DSCs were fabricated according to the following procedure. Firstly, polymer electrolytes were prepared by dissolving oligo-PEG (0.5 g; M_w = 1000 g/mol, Aldrich) in acetonitrile (9.5 g) as 5% (w/w) and then various contents of GA (50% in water, Aldrich) were added (as 13.0; 14.9; 16.7; 23.1% (w/w)). The mole ratio of potassium iodide to oxygen atom in PEG + GA blend (i.e., [–O–]:[–KI]) was varied as 10:1, 25:1, 35:1 and 50:1. Iodine was dissolved in the polymer solution as 10% for the solid weight of KI added. Small amount of HCl (<0.01% w/w) was added in polymer electrolyte solution to induce the crosslinking reaction [23]. All chemicals were purchased from Aldrich and utilized without further purifications. Transparent SnO_2:F-layered conductive glass (FTO, 8 Ω/γ, purchased from Pilkington) was employed to prepare the photo- and counter electrodes. For fabrication of photoelectrodes, firstly, Ti(IV) bis(ethyl acetoacetato)-diisopropoxide solution (2% w/w, in 1-butanol, Aldrich) was spin-coated onto FTO glass. The FTO glass was heated to 450 °C stepwise and sintered at 450 °C for 30 min. Then commercialized TiO_2 paste (Ti-Nanoxide T, Solaronix) was cast onto the FTO glass and sintered at 450 °C for 30 min. Nanocrystalline TiO_2 films (thickness of 11–34 μm) were sensitized with $Ru(dcbpy)_2(NCS)_2$ dye solution (535-bisTBA, Solaronix, 13 mg dissolved in distilled ethanol (50 g)) for overnight. Pt-layered counter electrodes were prepared by spin-coating of H_2PtCl_6 solution (0.05 mol dm^{-3} in isopropanol, Aldrich) onto FTO glass and successive sintering at 400 °C for 20 min. In this study, to improve the interfacial contact between the electrolyte and dye molecules, we have developed an effective preparation method (referred to as "multi-coating method") for preparing SDSCs. For the DSC fabrication, a dilute polymer electrolyte solution (1%, w/w) was first cast onto dye-adsorbed TiO_2 photoelectrode and allowed to be evaporated very slowly for complete penetration of polymer electrolytes through the void of nanopores. As a second step, a highly concentrated polymer electrolyte solution was cast onto the photoelectrode to minimize the time for evaporation of solvent as well as to prevent the formation of cavities between two electrodes during solvent evaporation. Then, Pt-layered FTO electrode was superposed upon it. The cells were then pressed between two glass plates in order to achieve the slow evaporation of solvent as well as to obtain a very thin SPE layer.

2.2. Morphological characterization

Morphological characterization for the nanocrystalline TiO_2 layer was carried out using a field-emission scanning electron microscope (FE-SEM, S-4700, Hitachi). The specific surface area of nanocrystalline TiO_2 film was evaluated by the Brunauer–Emmett–Teller (BET) method and the pore size distribution was also calculated from the N_2-desorption isotherm using the BJH method [30,31]. The average pore diameter was found to be around 16.5 nm and the surface area was 76.9 m^2/g.

2.3. Ion conductivity/FT-IR/FT-Raman/WAXS

Ionic conductivity was measured using a laboratory-made four-point probe conductivity cell connected to an impedance analyzer (IM6, ZAHNER). FT-IR measurements were performed on a 6030 Mattson Galaxy Series FT-IR spectrometer; 64–64 scans were signal-averaged at a resolution of 4 cm^{-1}. Spectroscopic characterization was performed using a pressure cell equipped with CaF_2 windows. FT-Raman spectra for polymer electrolytes were recorded at room temperature using a Perkin-Elmer System 2000 NIR FT-Raman at a resolution of 1 cm^{-1}. This experimental apparatus includes a neodymium-doped yttrium aluminum garnet (Nd^{3+}:YAG) laser operating at 1.064 μm. Wide angle X-ray scattering (WAXS) was performed

with Cu Kα radiation to characterize the structure of polymer electrolytes at a scanning speed of 5° min^{-1}.

2.4. Measurement of photovoltaic performances

The photovoltaic performances (short-circuit current J_{sc} (mA cm^{-2}), open-circuit voltage V_{oc} (V), fill factor ff and overall energy conversion efficiency η) were measured using a potentiostat/galvanostat (263A, EG&G Princeton Applied Research) under an illumination of 10–100 mW cm^{-2} (by a 150 W Xe lamp (Thermo Oriel Instruments)). The effective area of the test cell was 0.2 cm^2. The light intensity (or radiant power) was adjusted with a Si solar cell (Fraunhofer Institute for Solar Energy System; Mono-Si + KG filter; Certificate No. C-ISE269) for 1 sun light intensity (100 mW cm^{-2}) that was double-checked with a NREL-calibrated Si solar cell (PV Measurements Inc.) Moreover, the increase in temperature inside the cell during the measurement was prevented by using a cooler.

3. Results and discussion

3.1. Crosslinking of oligo-PEG

Oligo-PEG possessing hydroxyl (–OH) end groups can be crosslinked with GA via two possible reaction routes as shown in Fig. 1. As well known, GA can induce both the acetal linkage formation by a bifunctional reaction and aldehyde formation by a monofunctional reaction [23,32]. Fig. 2 shows the FT-IR spectra of neat PEG and PEG + KI/I_2 crosslinked with GA. With increasing the GA content, the O–H stretching vibration band at near 3387 cm^{-1} was decreased along with the band shift to a higher wavenumber at 3470–3432 cm^{-1}. This result suggests that the hydrogen bonding between –OH groups of PEG becomes weaker in crosslinked PEG than in neat PEG because

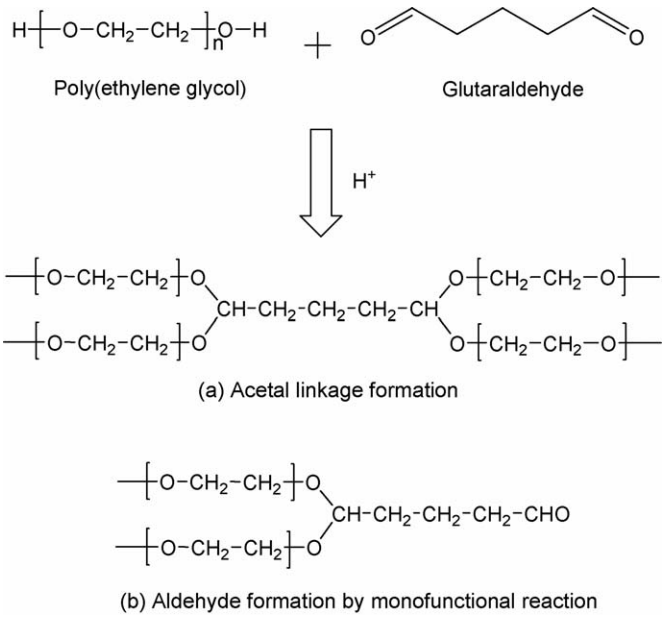

Fig. 1. Crosslinking scheme of poly(ethylene glycol) with glutaraldehyde.

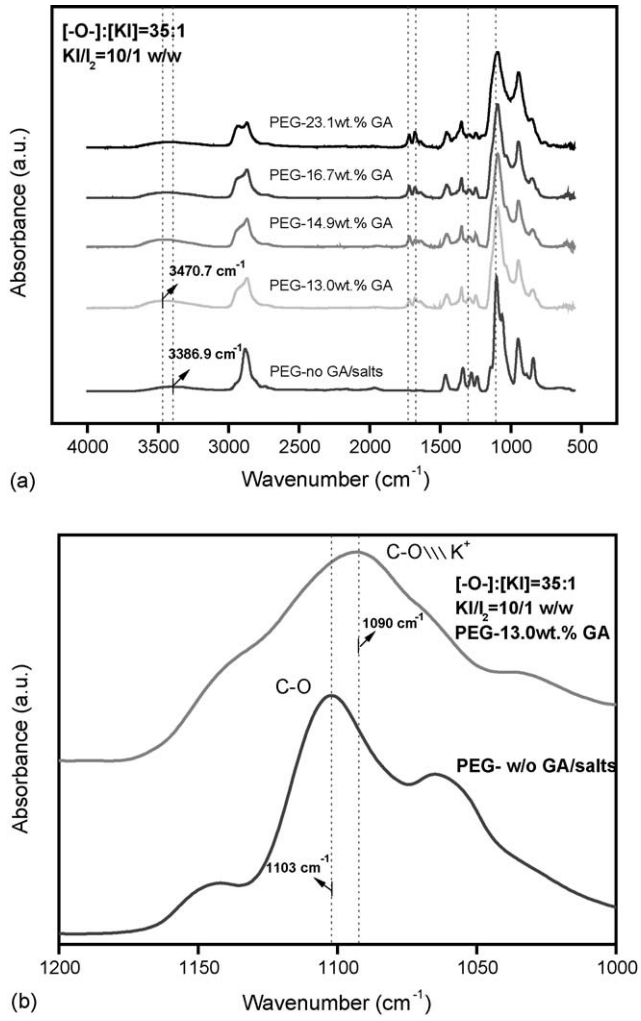

Fig. 2. FT-IR spectra of neat $PEG_{M_w=1000}$ (no salt) and crosslinked $PEG_{M_w=1000}/KI/I_2$ ([–O–]:[KI] = 35:1; KI/I_2 = 10/1 (w/w)) electrolyte with glutaraldehyde. (a) From 4000 to 500 cm^{-1}; (b) from 1200 to 1000 cm^{-1}.

of the diminution in the number of terminal –OH groups, indicating the chemical crosslinking of PEG with GA [23]. The absorption peak at near 1298 cm^{-1} was also observed in the spectra of PEG + GA, supporting the formation of ether bonds (C–O–C) between the hydroxyl groups of PEG and the aldehyde groups of GA. Eventually, it was confirmed that the terminal OH groups of oligo-PEG are chemically linked with the ether bond through acetalization [32]. However, the appearance of the aldehyde C=O bond at 1724 cm^{-1} with an addition of GA indicates that the aldehyde groups of GA do not completely react with –OH groups of PEG (i.e. monofunctional reaction), and the unreacted aldehyde groups are also available for the coordination with potassium ions [23]. The growth of absorption peak assigned to potassium-coordinated C=O bond at 1674 cm^{-1} with an addition of GA confirms the coordinative interaction between potassium ions and unreacted aldehyde groups. A lower peak position of coordinated C=O than free C=O (at 1724 cm^{-1}) is originated from the loosened interaction between carbon and oxygen resulting from the electron donation of oxygen to potassium cation [23]. The shift of C–O stretching peak in PEG

from 1103 to 1090 cm^{-1} (shown in Fig. 2(b)) upon the addition of potassium iodide also indicates the coordinative interaction between potassium and ether oxygen atom [20–23].

3.2. Structure of polymer electrolytes

WAXS spectra of PEG (w/o GA) and crosslinked PEG (w/GA) with and without the addition of KI/I_2 were obtained to investigate the structural change in the polymer electrolytes. The intensities in the several crystalline peaks of neat PEG observed at 19.2°, 23.4° and 26.7° drastically decrease upon addition of potassium iodide as shown in Fig. 3(a). Moreover, the crystalline peaks of solid KI and I_2 were not observed in the PEG electrolytes, indicating that the inorganic salts are completely dissolved in PEG. In the WAXS spectra of crosslinked PEG (shown in Fig. 3(b)), only broad amorphous hallow is observed irrespective of the GA concentrations. The value of Bragg *d*-spacing was calculated from the peak maximum using Bragg relation (i.e. $n\lambda = 2d\sin\theta$, here n is the positive integer, λ the wavelength, d the interplanar distance and θ is the angle from the crystal plane) and listed in Table 1. The result shows that the increases in the *d*-spacing with increasing the GA content added, indicating that the crosslinking agent (i.e. GA) also functions to enlarge the free volume of PEG even after solidification. The increase in the inter-chain distance of polymer medium possibly results in the enhancement of chain mobility for ion conduction.

Table 1
Bragg *d*-spacing of PEG + KI/I_2 and crosslinked PEG/GA + KI/I_2

Polymer electrolyte[a]	2θ (degree)	Bragg *d*-spacing (Å)
$PEG_{M_w=1000}$-No GA, KI/I_2	21.99	4.037
$PEG_{M_w=1000}$-13.0% (w/w) GA, KI/I_2	20.46	4.336
$PEG_{M_w=1000}$-14.9% (w/w) GA, KI/I_2	20.30	4.369
$PEG_{M_w=1000}$-16.7% (w/w) GA, KI/I_2	20.18	4.395
$PEG_{M_w=1000}$-23.1% (w/w) GA, KI/I_2	19.73	4.494

[a] [–O–]:[KI] = 35:1; KI/I_2 = 10/1 (w/w).

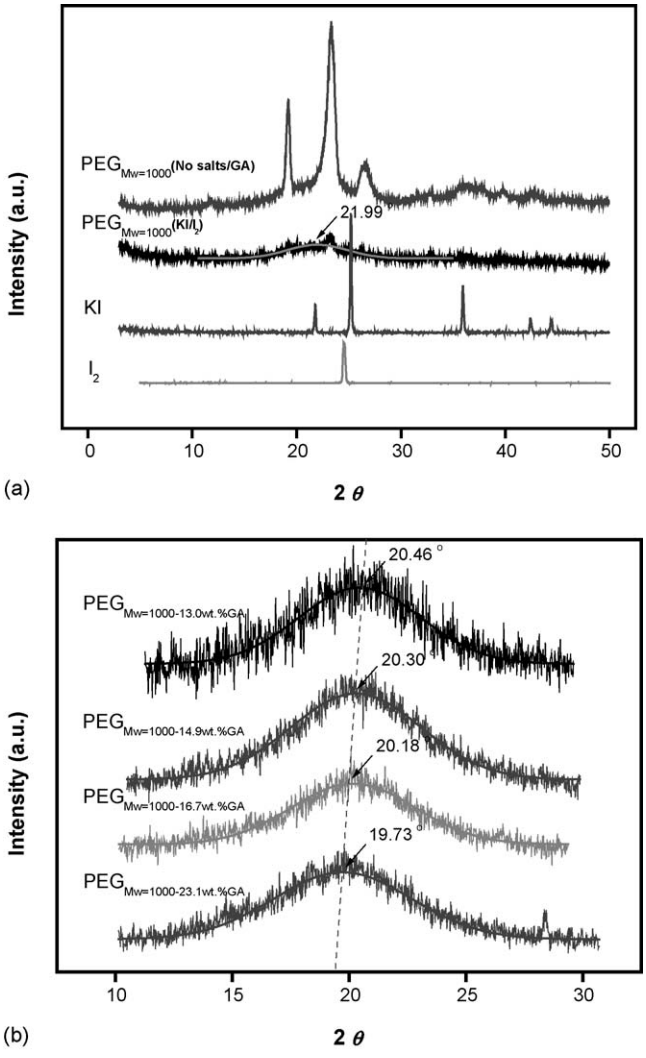

Fig. 3. WAXS spectra of crosslinked $PEG_{M_w=1000}/KI/I_2$ ([–O–]:[KI] = 35:1; KI/I_2 = 10/1 (w/w)) electrolytes with different GA contents. (a) Neat PEG, PEG/KI/I_2 (w/o GA), KI and I_2; (b) PEG/KI/I_2 (w/ GA).

3.3. Dissolution of KI and I_2

FT-Raman spectra were obtained to confirm the formation of I_3^- and polyiodides (I_{2n+3}^-, here n = 1, 2, 3, . . .) and the complete dissolution of iodine in solid-state polymer electrolytes. Recently, it has been demonstrated the formation of I_3^- and polyiodides in liquid and gel electrolytes containing iodide and iodine [13]. Their results showed that iodines are completely dissolved to form I_3^- and polyiodides, and also the Grotthuss-type iodide transport is induced in both liquid and gel electrolytes. Similarly, for the oligo-PEG/GA + KI/I_2 electrolytes, two symmetric stretching peaks assigned to I_3^- at around 113 cm^{-1} and polyiodides (e.g. I_5^-) at around 141 cm^{-1} were observed as shown in Fig. 4. However, the intensity of the former peak is much higher than that of the latter, demonstrating that iodide species are present mostly as I_3^-. Moreover, the band attributed to vibration of molecular iodine around 180–210 cm^{-1} was not observed, confirming the complete dissolution of I_2 in solid-state PEG/GA + KI/I_2 electrolytes [13,33].

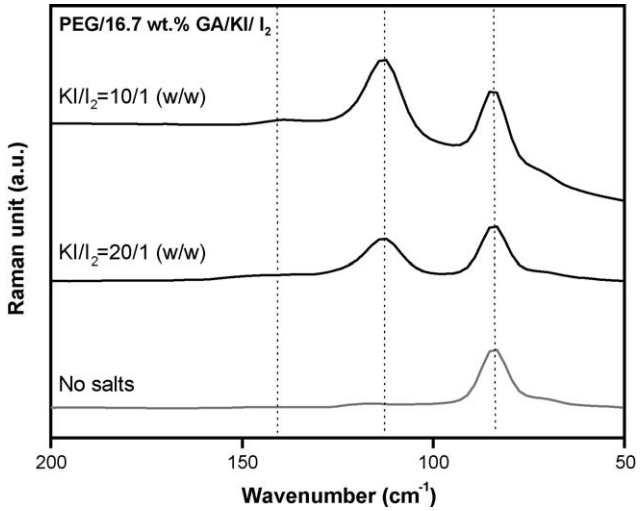

Fig. 4. FT-Raman spectra of neat $PEG_{M_w=1000}$ (no salt) and crosslinked $PEG_{M_w=1000}/KI/I_2$ ([–O–]:[KI] = 35:1) electrolytes with glutaraldehyde.

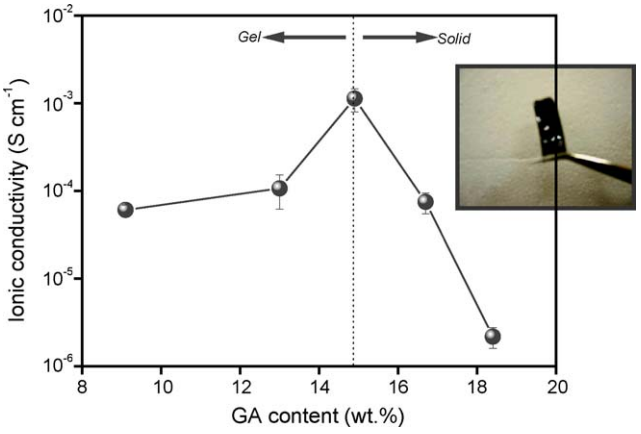

Fig. 5. Ionic conductivities of crosslinked $PEG_{M_w=1000}$/KI/I_2 ([–O–]:[KI] = 35:1; KI/I_2 = 10/1 (w/w)) electrolytes by varying the GA content measured at 25 °C, [H_2O] < 1 ppm.

3.4. Ionic conductivity

The ionic conductivities of the crosslinked oligo-PEG electrolytes are shown in Fig. 5 as a function of the GA content. The solidifying point of the oligo-PEG/GA system was observed at the GA content of ca. 15% (w/w) (the picture embedded in Fig. 5 shows the solidified film of crosslinked oligo-PEG electrolyte). The ionic conductivities gradually increase with the increase in the GA content up to solidifying point, above which they decrease. The increase in the ionic conductivity seems to be owing to the enhanced chain mobility of PEG by the increase in the inter-chain distance and consequently free volume with the increase in the amount of GA as confirmed by WAXS. The decrease in ionic conductivity above the maximum point may result from the reduced chain flexibility due to the solidification of polymer matrix. At the maximum point, the ionic conductivity of the electrolyte is as high as 10^{-3} S cm^{-1} at room temperature.

3.5. Penetration of polymer electrolytes into TiO_2 layer

The deep penetration of the oligo-PEG based electrolyte into the nanoporous TiO_2 layer was confirmed by the cross-sectional FE-SEM images of the photoelectrode. Fig. 6 shows the cross-sectional FE-SEM images of the nanoporous TiO_2 layers coated with: (a) high molecular weight PEO + KI/I_2 and (b) crosslinked oligo-PEG/GA + KI/I_2 electrolytes. When high molecular weight PEO (M_w = 1,000,000 g/mol and R_g = 63 nm) was cast, nanocrystalline TiO_2 particles maintain their original size (i.e. diameter = 20–30 nm) and shape, and do not seem to be adequately coated with polymer electrolytes as shown in Fig. 6(a), suggesting insufficient penetration of electrolyte materials into the nanopores (average pore diameter = 16.5 nm) and therefore poor contact between electrolytes and TiO_2 nanoparticles [26–28]. In the case of oligo-PEG/GA + KI/I_2 (M_w of PEG = 1000 g/mol and R_g = 2 nm), the dramatic improvement in the interfacial contact between TiO_2 particles and electrolytes is evident as shown in Fig. 6(b).

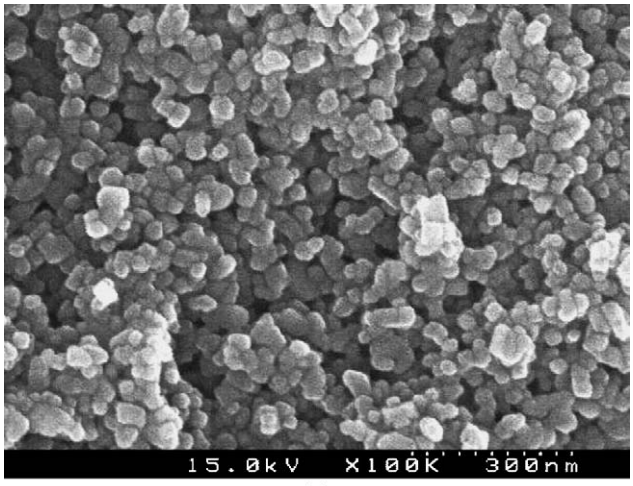

(a)

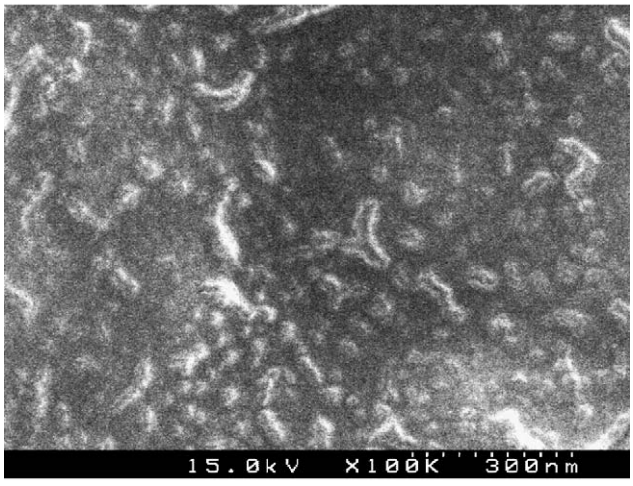

(b)

Fig. 6. Cross-sectional FE-SEM images for nanocrystalline TiO_2 layers incorporated with PEO: (a) $PEO_{M_w=1,000,000}$/KI/I_2 ([–O–]:[KI] = 35:1; KI/I_2 = 10/1 (w/w)) (η = 0.01% at 100 mW cm^{-2}) and (b) crosslinked $PEG_{M_w=1000}$/KI/I_2 with glutaraldehyde (η = 2.30% at 100 mW cm^{-2}).

3.6. Solar energy conversion performance

The photovoltaic performances of SDSCs prepared using crosslinked PEG electrolytes have been evaluated by means of *J–V* measurements. The fill factor (ff) and overall energy conversion efficiency (η) were calculated by the following equations:

$$\mathrm{ff} = \frac{V_{max} \cdot J_{max}}{V_{oc} \cdot J_{sc}} \quad (1)$$

$$\eta(\%) = \frac{V_{max} \cdot J_{max}}{P_{in}} \times 100 = \frac{V_{oc} \cdot J_{sc} \cdot \mathrm{ff}}{P_{in}} \times 100 \quad (2)$$

where J_{sc} is the short-circuit current (mA cm^{-2}), V_{oc} the open-circuit voltage (V), P_{in} the incident light power and J_{max} (mA cm^{-2}) and V_{max} (V) is the current and voltage in the *J–V* curve (V), respectively, at the point of maximum power output.

We have fabricated the SDSCs with varying the thickness from 11 to 34 μm of the nanoporous TiO_2 layer to optimize the energy conversion efficiency and results are summarized in

Table 2
Photovoltaic characteristics of open-circuit voltage (V_{oc}), short-circuit current (J_{sc}), fill factor (ff) and overall energy conversion efficiency (η) for the SDSCs employing crosslinked $PEG_{M_w=1000}$/KI/I_2 electrolyte measured with glutaraldehyde under 100 and 10 mW cm^{-2} illuminations

Electrolyte	Thickness of TiO_2 layer (μm)[a]	V_{oc} (V)[b]	J_{sc} (mA cm^{-2})[b]	ff (−)[b]	η (%)[b]	η (%)[c]
$PEG_{M_w=1000}$-GA (14.9 wt.%)/KI/I_2	11	0.58	4.02	0.66	1.54	7.23
	21	0.54	4.86	0.62	1.63	7.38
	25	0.59	5.03	0.65	1.93	8.12
	34	0.62	6.05	0.61	2.30	9.45

[a] Estimated from the cross-sectional FE-SEM images.
[b] Measured at 100 mW cm^{-2}.
[c] Measured at 10 mW cm^{-2}.

Table 2. J_{sc} increases to a large extent with the thickness of the TiO_2 layer, whereas V_{oc} and ff do not. The increase in J_{sc} with the increase in the TiO_2 thickness suggests that the amount of generated electrons is increased due to the large amount of dye molecules adsorbed on the nanoporous TiO_2 layer. Interestingly, the energy conversion efficiency at weak illumination is exceptionally high, and the large difference in the efficiencies measured at strong (i.e. 100 mW cm^{-2}) and at weak illuminations (i.e. 10 mW cm^{-2}) was observed. This result suggests that the mass transfer rate of I_3^- through the solid polymer electrolyte could be a major rate-limiting step under strong illumination. As shown in Fig. 7, the overall energy conversion efficiencies for SDSCs also depend on the mole ratio of potassium iodide to oxygen. The optimal salt content of around [–O–]:[KI] = 35:1 showed the highest efficiency $\eta = 2.30\%$ at 1 sun (AM1.5). In this work, moreover, the photovoltaic performance has been more improved by means of the introduction of chemically doped (p-type, with I_2) conjugated polymer (poly(2-methoxy-5-(2′-ethylhexyloxy)-1,4-phenylenevinylene) (MEH-PPV)) thin-layer onto a conventional Pt-layered electrode as revealed in Fig. 8. The overall conversion efficiency was increased to a large extent upon the insertion of MEH-PPV:I_3^- junction layer on the counter electrode mostly due to the enhancements in the photocurrent and the fill factor. This result indicates that the iodine-doped conjugated polymer coated on the electrode

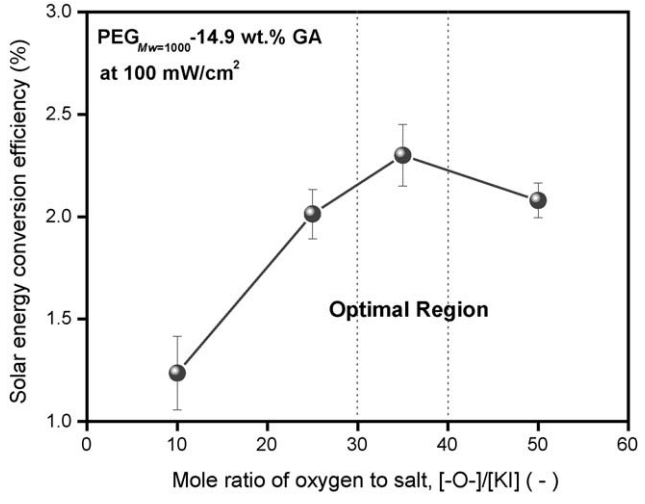

Fig. 7. Overall solar energy conversion efficiencies of SDSCs employing crosslinked $PEG_{M_w=1000}$/KI/I_2 ([–O–]:[KI] = 35:1; KI/I_2 = 10/1 (w/w)) electrolyte with glutaraldehyde.

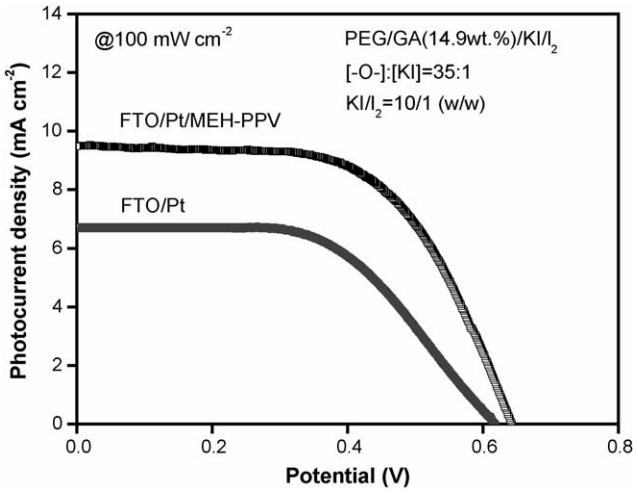

Fig. 8. J–V curves of DSCs ($t_{TiO_2} = 34$ μm) employing crosslinked $PEG_{M_w=1000}$/KI/I_2 ([–O–]:[KI] = 35:1; KI/I_2 = 10/1 (w/w)) electrolyte with glutaraldehyde measured under 100 mW cm^{-2} illumination.

significantly decreases the electron transfer resistance at the interface between platinum catalyst and triiodide dissolved in polymer medium owing to the affinity for both I_3^- ions and electrons of the junction layer. The best result of the SDSC incorporating crosslinked oligo-PEG/GA + KI/I_2 electrolyte and counter electrode with MEH-PPV:I_3^- junction layer exhibits J_{sc} of 9.48 mA cm^{-2}, the V_{oc} of 0.64 V, the ff of 0.60 and the η of 3.64% at 100 mW cm^{-2}. More details of the MEH-PPV:I_3^- junction layer will be reported in our other publications.

4. Conclusion

Highly efficient SDSCs have been successfully prepared by employing oligo-PEG + KI/I_2 electrolyte crosslinked with bifunctional glutaraldehyde. The improved efficiency has been achieved by both the enlarged interfacial contact between electrolyte and dye molecules and the high ionic conductivity of the electrolyte. The enlarged interfacial contact is associated with the deeper penetration of the electrolyte solution into the nanoporous TiO_2 layer because of the smaller coil size of oligo-PEG compared to the average pore diameter of the nanoporous TiO_2 layer. The crosslinked oligo-PEG/GA + KI/I_2 electrolytes also show the reasonably high ionic conductivity (i.e. 10^{-3} to 10^{-5} S cm^{-1}). Therefore, the high conversion efficiency of 3.64% at 100 mW cm^{-2} has been achieved for the SDSCs.

References

[1] B. O'Regan, M. Grätzel, Nature 353 (1991) 737.
[2] U. Bach, D. Lupo, P. Comte, J.E. Moser, F. Weissörtel, J. Salbeck, H. Spreitzer, M. Grätzel, Nature 395 (1998) 583.
[3] K. Hara, T. Sato, R. Katoh, A. Furube, Y. Ohga, A. Shinpo, S. Suga, K. Sayama, H. Sugihara, H. Arakawa, J. Phys. Chem. B 107 (2003) 597.
[4] S. Ferrere, B.A. Gregg, J. Phys. Chem. B 105 (2001) 7602.
[5] N.-G. Park, J. van de Lagemaat, A.J. Frank, J. Phys. Chem. B 104 (2000) 8989.
[6] M. Grätzel, J. Photochem. Photobiol. A: Chem. 164 (2004) 3.
[7] R.F. Service, Science 300 (2003) 1219.
[8] A.F. Nogueira, J.R. Durrant, M.-A. De Paoli, Adv. Mater. 13 (2001) 826.
[9] T. Stergiopoulos, I.M. Arabatzis, G. Katsaros, P. Falaras, Nano Lett. 2 (2002) 1259.
[10] G. Katsaros, T. Stergiopoulos, I.M. Arabatzis, K.G. Papadokostaki, P. Falaras, J. Photochem. Photobiol. A: Chem. 149 (2002) 191.
[11] M. Grätzel, Prog. Photovolt. Res. Appl. 8 (2000) 171.
[12] W. Kubo, S. Kambe, S. Nakade, T. Kitamura, K. Hanabusa, Y. Wada, S. Yanagida, J. Phys. Chem. B 107 (2003) 4374.
[13] W. Kubo, K. Murakoshi, T. Kitamura, S. Yoshida, M. Haruki, K. Hanabusa, H. Shirai, Y. Wada, S. Yanagida, J. Phys. Chem. B 105 (2001) 12809.
[14] E. Stathatos, P. Lianos, U. Lavrencic-Stangar, B. Orel, Adv. Mater. 14 (2002) 354.
[15] O.A. Ileperuma, M.A.K.L. Dissanayake, S. Somasundaram, Electrochim. Acta 47 (2002) 2801.
[16] D. Gebeyehu, C.J. Brabec, N.S. Sariciftci, D. Vangeneugden, R. Kiebooms, D. Vanderzande, F. Kienberger, H. Schindler, Synth. Met. 125 (2002) 279.
[17] D. Gebeyehu, C.J. Brabec, N.S. Sariciftci, Thin Solid Films 403 (2002) 271.
[18] P. Wang, S.M. Zakeeruddin, J.E. Moser, M.K. Nazeeruddin, T. Sekiguchi, M. Gratzel, Nat. Mater. 2 (2003) 402.
[19] S. Sakaguchi, H. Ueki, T. Kato, T. Kado, R. Shiratuchi, W. Takashima, K. Kaneto, S. Hayase, J. Photochem. Photobiol. A: Chem. 164 (2004) 117.
[20] J.H. Kim, B.R. Min, C.K. Kim, J. Won, Y.S. Kang, Macromolecules 35 (2002) 5250.
[21] J.H. Kim, B.R. Min, C.K. Kim, J. Won, Y.S. Kang, J. Phys. Chem. B 106 (2002) 2786.
[22] J.H. Kim, B.R. Min, J. Won, Y.S. Kang, Macromolecules 36 (2003) 4577.
[23] J.H. Kim, B.R. Min, K.B. Lee, J. Won, Y.S. Kang, Chem. Commun. (2002) 2732.
[24] G. Mao, R.F. Perea, W.S. Howells, D.L. Price, M.L. Saboungi, Nature 405 (2000) 163.
[25] Z. Gadjourova, Y.G. Andreev, D.P. Tunstall, P.G. Bruce, Nature 412 (2001) 520.
[26] Y.J. Kim, J.H. Kim, M.-S. Kang, M.J. Lee, J. Won, J.C. Lee, Y.S. Kang, Adv. Mater. 16 (2004) 1753.
[27] J.H. Kim, M.-S. Kang, Y.J. Kim, J. Won, N.-G. Park, Y.S. Kang, Chem. Commun. (2004) 1662.
[28] M.-S. Kang, J.H. Kim, Y.J. Kim, J. Won, N.-G. Park, Y.S. Kang, Chem. Commun. (2005) 889.
[29] C. Vandermiers, P. Damman, M. Dosière, Polymer 39 (1998) 5627.
[30] S. Brunauer, P.H. Emmett, E. Teller, J. Am. Chem. Soc. 60 (1938) 309.
[31] E.P. Barret, L.G. Joyner, P.P. Halenda, J. Am. Chem. Soc. 73 (1951) 373.
[32] C.-K. Yeom, K.-H. Lee, J. Membr. Sci. 109 (1996) 257.
[33] P. Klaeboe, J. Am. Chem. Soc. 89 (1967) 3667.